Nigerian Journal of Technology (NIJOTECH)
Vol. 44, No. 1, March, 2025, pp.17 - 28
www.nijotech.com

Print ISSN: 0331-8443
Electronic ISSN: 2467-8821
https://doi.org/10.4314/njt.v44i1.3

PROPERTIES ENHANCEMENT AND COMPOSITIONAL OPTIMIZATION STUDY OF TAILORED NANOSILICA REINFORCED BIOPLASTIC FILM COMPOSITES

AUTHORS:
H. Onovo[1,*], A. Agbeleye[2], T. Akano[3], K. Orafunam[4], D. Oludele[5], J. Olawoyin[6], and I. Kentosu[7]

AFFILIATIONS:
[1,2,4,5,6,7]Department of Metallurgical and Materials Engineering, University of Lagos, Nigeria
[3]Department of Mechanical Engineering, University of Botswana Gaborone, Botswana

***CORRESPONDING AUTHOR:**
Email: honovo@unilag.edu.ng

ARTICLE HISTORY:
Received: 11 November, 2024.
Revised: 24 March, 2025.
Accepted: 26 March, 2025.
Published: 14 April, 2025.

KEYWORDS:
Bioplastic film composite, Starch, Glycerol, Silicate nanoparticle, Maximum Biodegradability, Water absorption, Optimal performance, Tensile strength, Hydrophilicity, Tensile modulus, Sustainable.

ARTICLE INCLUDES:
Peer review

DATA AVAILABILITY:
On request from author(s)

EDITORS:
Chidozie Charles Nnaji
Ozoemena Anthony Ani

FUNDING:
None

Abstract

The harmful environmental impact of synthetic plastics has created an urgent need to develop biodegradable polymers for industrial and commercial applications. This study developed sustainable bioplastic film composites from renewable starch and SiO_2 nanoparticles (SiO_2-NPs) as alternatives to conventional plastics. The films were fabricated by varying the proportions of starch, glycerol, and SiO_2-NPs, and standard tests measured biodegradability, water absorption, and tensile strength. Surface plot analysis and regression models correlated composition with performance, enabling the identification of optimal formulations for applications such as food packaging and medical devices. Results showed that biodegradability and water absorption increase with higher starch and glycerol levels but decrease with more SiO_2-NPs, while tensile strength and modulus improve with increased SiO_2-NPs yet decline with higher starch and glycerol. Optimal performance was achieved at distinct compositions: maximum biodegradability (>70%) and highest tensile strength (1.6 MPa) were observed at 13–14% SiO_2-NPs and 1–2% starch, whereas minimum water absorption (20–60%) occurred at 0–1% SiO_2-NPs and 13–14% starch. These findings indicate that the total amounts of SiO_2-NPs and starch, rather than their ratio, predominantly control the film properties. For instance, films with 11 g starch, 9.15 g glycerol, and 2 g SiO_2-NPs exhibited 9.8% biodegradability, while those with 13 g starch, 9.15 g glycerol, and 1.2 g SiO_2-NPs showed 9.2%, suggesting that increased glycerol and SiO_2-NPs reduce biodegradability. Similarly, higher starch and glycerol elevate water absorption due to starch's hydrophilicity, though added SiO_2-NPs lowered it, and tensile strength improves with more SiO_2-NPs while declined with increased starch and glycerol. Results also specified that the bioplastic films had an average thickness of 0.4 mm, their density increased linearly with the SiO_2-NPs additions, and they achieved V-1 and V-2 flammability ratings. Thus, adjusting these components tailored the bioplastic films for specific applications, supporting their development as sustainable alternatives to conventional plastics.

1.0 INTRODUCTION

The growing utilization of petrochemical-derived synthetic plastics has given rise to significant concerns encompassing health, environmental impact, and economic ramifications [1]. While various techniques like recycling, reusing, and incineration have been employed to mitigate the adverse effects, they fall short of eliminating harmful compounds, non-biodegradability, and contributing to environmental pollution. Consequently, concerted efforts are underway to reduce the consumption of these plastics. Alternatively, a partial solution to the predicament of accumulating solid waste comprising inert synthetic

HOW TO CITE:
Onovo, H., Agbeleye, A., Akano, T., Orafunam, K., Oludele, D., Olawoyin, J., and Kentosu, I. "Properties Enhancement and Compositional Optimization Study of Tailored Nanosilica Reinforced Bioplastic Film Composites", *Nigerian Journal of Technology*, 2025; 44(1), pp. 17 – 28; *https://doi.org/10.4314/njt.v44i1.3*

polymers is the utilization of biodegradable polymers for packaging [2]. Starch, abundant and cost-effective, has found application in the realm of biomaterials. Starch films utilization represents a prudent harnessing of natural resources, and helps in averting pollutions arising from the environment. Starch-based films offer numerous advantages, including renewability, cost-effectiveness, ease of production, and biodegradability. Extensive research has been dedicated to the development of polymers derived from starch to preserve petrochemical resources and minimize environmental impact. However, it's important to note that starch-based materials exhibit certain drawbacks, such as stability in the long time, aging, and suboptimal mechanical properties [3, 4]. To address these limitations, plasticizers like glycerin have been incorporated to enhance shelf-life, elasticity, and overall product performance [5]. Plasticized starch, a versatile derivative of starch, exhibits remarkable adaptability and can be blended with a diverse range of polymeric materials to cater to a wide spectrum of applications. Researchers have delved into various modification techniques, encompassing derivatization, graft copolymerization, and blending, to refine and enhance the properties of starch bioplastic, leading to a material with improved performance and expanded applicability.

The potential to modify starch with SiO_2-NPs of 2.4 g/cm^3 density, arises from its multi-hydroxyl properties and high surface activity. This combination results in an interpenetrating structure of networks associated with SiO_2-NPs/starch hybrid materials, blending the rigidity of SiO_2-NPs with the flexibility of starch. Existing studies have demonstrated the ability of nanomaterials to improve the performance of polymer materials like plastics and rubber [6]. Nevertheless, no pertinent research has yet delved into producing and optimizing polymers derived from sweet potato starch adapted by SiO_2-NPs. This study focuses on amalgamating sweet potato starch with varying quantities of SiO_2-NPs. The primary objective is to create biodegradable films and optimize their biodegradability, tensile strength, and water absorption capacity within the context of SiO_2-NPs/starch-based biodegradable biopolymer films. Furthermore, various tests will be conducted, including FTIR, TGA, and SEM.

2.0 MATERIALS AND METHOD

2.1 Materials

SiO_2-NPs with a particle size of 50 nm were procured from a Chinese supplier, white flesh sweet potatoes were obtained from the Mushin market in Lagos, Nigeria, distilled water was acquired from the Metallurgical and Materials Engineering Laboratory at the University of Lagos, while glycerol and acetic acid were purchased from a chemical store in Ojota, Lagos, Nigeria.

2.2 Methods

2.2.1 Starch extraction and composite bioplastic film preparation

The sweet potatoes were peeled, cut, and soaked to soften for grinding. They were then washed, rinsed, and ground in batches using a hand blender. The resultant blend was mixed with water, and sieved to separate the starch-rich water from the solids. After settling for eight hours, the water was decanted and the starch dried using air and sun. The starch bioplastic film (SBF) was prepared by adding starch to distilled water (100 mL) and stirring for 5 min. The blend was heated at 200 °C with stirring via an epoxy mixer attached to a hand drill machine. After 10 min, glycerol was added and stirred for 5 min, then acetic acid (which straightens amylopectin into amylose) was added and stirred for 10 min. The blend was poured onto an 8 cm × 11 cm wooden surface and oven-dried (NLO-2000, 220V, 50-60Hz, 1ph) at 100 °C for 2 hours before the films were extracted. For the composite biopolymer film (CBF 1), SiO_2-NPs were dispersed in distilled water (100 mL), and stirred for 5 min. Starch was added, stirred for 5 min more, and then heated to 200 °C with continuous mechanical agitation. This procedure was repeated seven times with varying amounts of starch, SiO_2-NPs, glycerol, and acetic acid. The experimental design used open-source Scilab-2024, details are in Table 1.

Table 1: Experimental design

Composite	Run order	Starch (g)	SiO_2-NPs (g)	Glycerol (g)	Acetic acid (g)
SBF	1	15.000	0.000	10.000	10.000
CBF1	2	14.375	0.625	9.375	10.625
CBF2	3	13.750	1.250	10.625	9.375
CBF3	4	13.125	1.875	9.375	10.625
CBF4	5	12.500	2.500	10.00	10.000
CBF5	6	11.875	3.125	10.625	9.375
CBF6	7	11.250	3.750	10.625	9.375
CBF7	8	10.625	4.375	9.375	10.625
CBF8	9	10.000	5.000	10.000	10.000

2.2.2 Experimental design optimization

Adapted Minitab was used for experimental design and optimization via mixture design, RSM, and ANOVA to determine the optimal starch and SiO_2-NPs composition. Data were processed with regression for mixtures, while ANOVA targeted water absorption (%), biodegradability (%), and tensile strength (MPa) using a "larger is better" criterion, which indicates a preference for higher value. Response surface plots illustrate the effects and interactions of starch and SiO_2-NPs on film

performance. Multi-response, multi-factor optimization was performed using a response surface optimizer (RSO) based on the Derringer-modified Harrington's desirability function approach. This method converts each response into a desirability value (0–1) and maximizes overall desirability to identify optimal factor settings.

2.2.3 Film thickness measurement

Measurements of the film thickness were done using a high-precision micro-meter (0.001 mm resolution). Three random measurements per film ensured data integrity. These values were statistically analyzed, with the arithmetic mean reliably representing each film's thickness.

2.2.4 Specific gravity and density

Bioplastic films (10 cm × 1 cm) were used to determine specific gravity per ASTM D792-07. Each film's mass in the air was measured using a digital scale (0.1 mg precision). Films were submerged in purified water to record the apparent mass. Specific gravity was calculated using Equation 1.

$$\text{Specific gravity} = a/(a + w - b) \quad (1)$$

Where *a*, *b* and *w*, are the mass in air, apparent mass of the fully submerged sample (with partly immersed wire), and apparent mass of the wire, respectively. Density was calculated from specific gravity using Equation 2. This method connects film measurements to density, ensuring reliable characterization of the bioplastic films (ASTM D792-07).

$$\text{D} = \text{Specific gravity} * 997.6\ (\text{kg/m}^3) \quad (2)$$

2.2.5 Flammability test

This test determines the self-extinguishing time of a vertically mounted polymer specimen by clamping its top and positioning a burner directly beneath it. Conducted following ASTM D792-07, the test measures burning and afterglow durations, as well as dripping. Materials are rated as follows: V-0 if the flame extinguishes in under 10 seconds with no dripping; V-1 if in under 30 seconds with no dripping; and V-2 if in under 10 seconds despite dripping.

2.2.6 Tensile test

The tensile properties of the bioplastic films were assessed using a Universal Tensile Machine (UTM-D2) per ASTM D882-10, with a crosshead speed of 1 mm/min. Samples measuring 80 mm by 20 mm were preconditioned in the lab for approximately 40 hours at 22 °C.

2.2.7 Water absorption

Following ASTM D570-98, water absorption was measured on 75 mm × 30 mm specimens over seven days in purified water at room temperature (due to the swelling tendencies that reach maximum around this period). Each specimen's initial weight was recorded with 0.01 g precision. After 24 hours of submersion, excess water was removed before re-weighing. Absorption was calculated with Equation 3.

$$M(\%) = (m_t - m_o)/m_o * 100 \quad (3)$$

Where m_o is the initial oven-dry weight and m_t is the weight after time t. This method connects precise weight measurements to water uptake over time.

2.2.8 Fourier-transform infrared spectroscopy (FTIR)

FTIR was conducted using a PerkinElmer FTIR spectrophotometer. FTIR analysis allowed for the detection of functional groups in the films. IR Prestige-21 Shimadzu was used to perform the FTIR spectroscopy. These analyses were performed on all the bioplastic films.

2.2.9 Thermogravimetric analysis (TGA)

TGA was performed with a PerkinElmer TGA 4000 instrument under a nitrogen atmosphere. The analysis determined the thermal degradation characteristics of the biodegradable films.

2.2.10 Biodegradability

The biodegradability rate was assessed using a desiccator. Three specimens per sample were weighed before placement and again after 24 hours. This procedure was repeated over seventeen days (because two "bio -deterioration and -fragmentation" out of three main stages of biodegradation must have been completed), and the average weight change was computed to determine biodegradability.

2.2.11 Morphological examination

Microstructural analysis of the bioplastic films was performed using a Zeiss Merlin SEM per ASTM E766-14e1, which standardizes specimen preparation for accurate results. Surface and cross-section images were captured at 1500x magnification, revealing detailed topography, pore structure, and reinforcing agent distribution. This method confirms SEM's power in elucidating film morphology and microstructural features.

3.0 RESULTS AND DISCUSSION

3.1 Film Thickness Measurement

The bioplastic films formed an average of 0.4 mm as presented in Figure 1, indicating that the films produced can produce carrier bags. This is an

improvement to a previous study by [7] which produced an average of 0.316 mm. The higher thickness values can be attributed to the presence of more SiO_2-NPs.

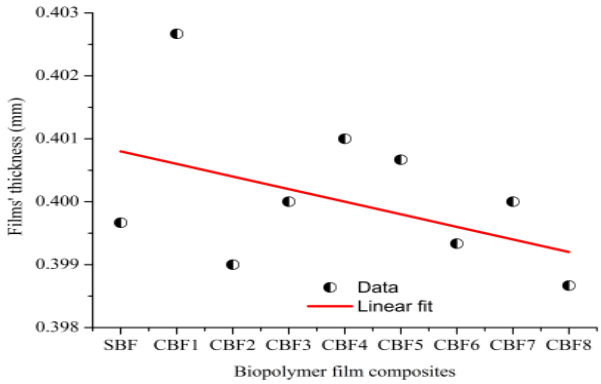

Figure 1: The thickness of bioplastic films investigated

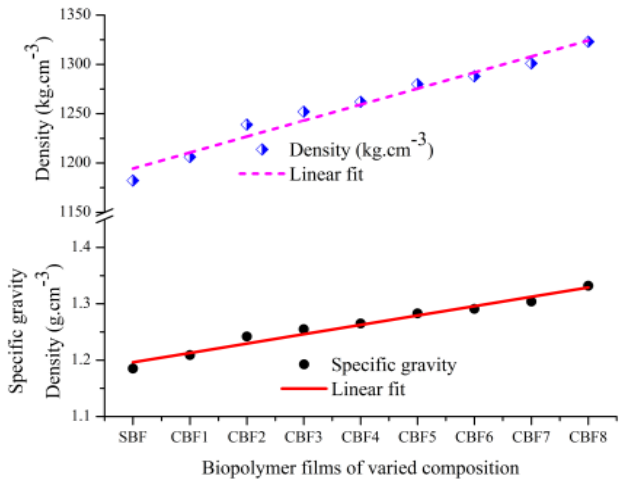

Figure 2: Biopolymer film composites with different specific gravity same as density in g.cm^{-3}, and density in kg.cm^{-3}

3.2 Specific Gravity and Density

The specific gravity of the bioplastics as an average of the test specimens is represented in Figure 3, together with the density of the bio-plastic films calculated using the ASTM D792-07 standard Equation 2 and as also shown in Figure 2. The specific gravity and density of bioplastic film composites exhibit a linear connection with SiO_2-NPs addition.

3.3 Flammability Test

The specimen is clamped, with a burner placed beneath to assess flammability (burning, afterglow, and dripping) and fire propagation. Figure 3 shows the self-extinguishing time of a vertically oriented biopolymer specimen. Conventional polyethylene failed the UL-94 test—it ignited within 10 s and burned completely due to high flammability and dripping. In contrast, SiO_2-NPs starch-based films formed a char coating that isolated the sample, extinguishing flames in under 30 s per application. Although these films dripped after a second flame application (igniting the cotton below), they achieved V-1 and V-2 ratings. CBF3, CBF6, CBF7, and CBF8 performed better than SBF, indicating that SiO_2-NPs enhance flame resistance, while CBF1, CBF2, CBF4, and CBF5 did not improve due to composite defects.

This study shows that SiO_2-NPs enhance the flame resistance of starch-based biopolymers.

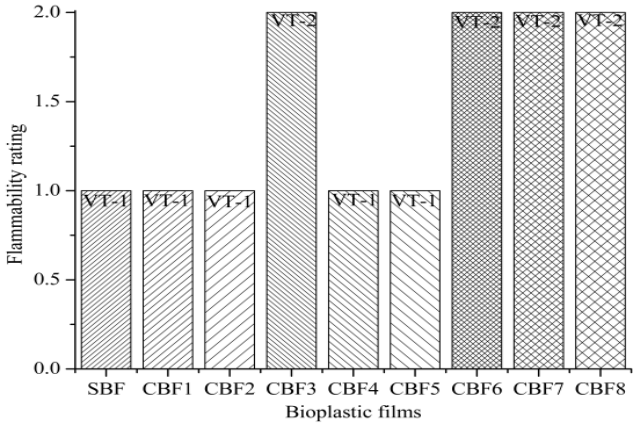

Figure 3: The behavior of fire (UL-94) on SBF and CBFs biopolymer

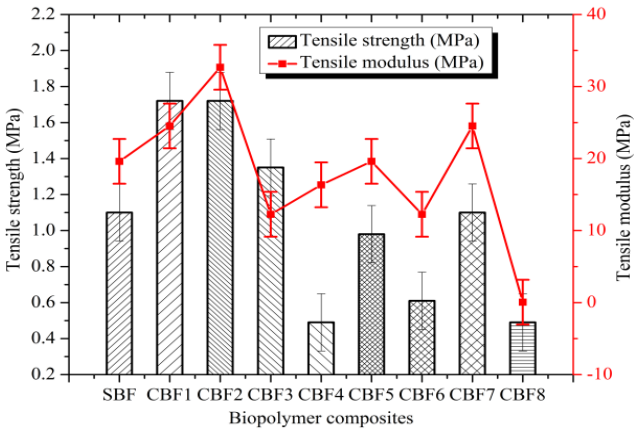

Figure 4: Biopolymer film composites' tensile strength and modulus of elasticity with SiO_2-NPs addition

3.4 Tensile Property

Figure 4 show the tensile test results, highlighting the impact of SiO_2-NPs on film strength. The pure starch film (SBF) had a tensile strength of 1.10 MPa. Adding SiO_2-NPs increased strength up to 1.81 MPa before fluctuations occurred, suggesting that excessive nanoparticles induce irregularities. SEM micrographs confirmed these irregularities, likely due to unsystematic microstructure and additive composition. [8] reported that plasticizers improve film

flexibility and workability, which supports these findings. Overall, tensile strengths ranged from 0.49 to 1.81 MPa, with CBF1, CBF2, and CBF3 showing superior strength and modulus compared to SBF.

Specifically, their tensile moduli were 24.52, 32.67, and 12.26 MPa, and elongations at break were 12.00%, 12.75%, and 5.00%, versus SBF's 19.61 MPa and 5.60%. These results indicate that optimized SiO_2-NPs levels enhance mechanical properties, while excessive addition may compromise structural integrity.

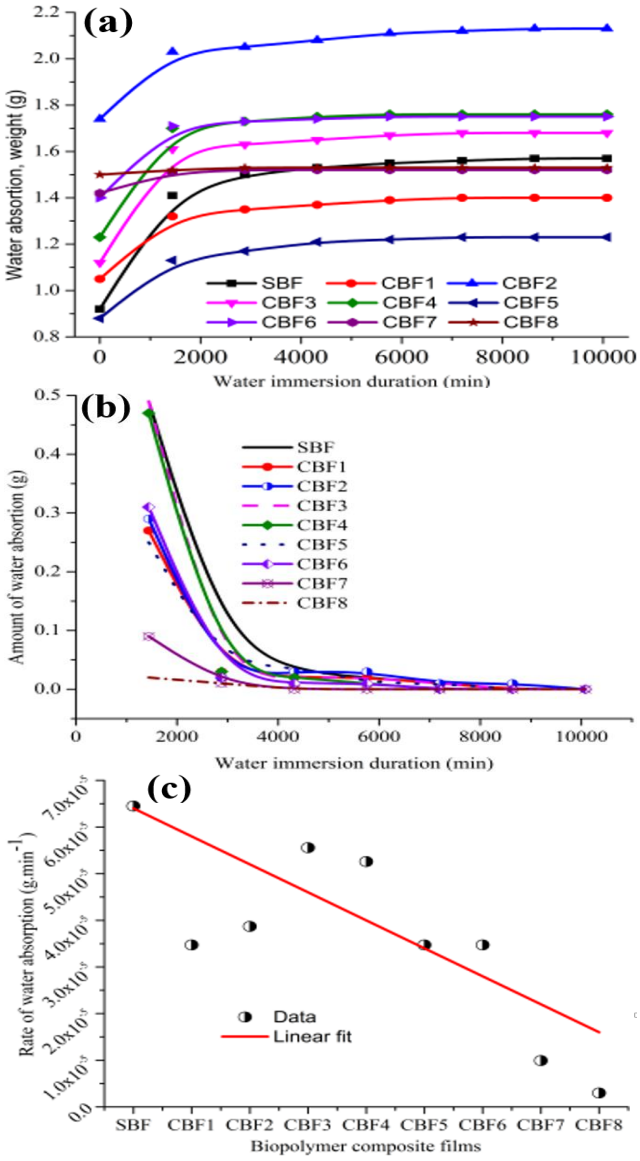

Figure 5: Water intake of biopolymer film composites: **(a)** water absorption profile, **(b)** amount of water absorbed at 1440-min intervals, and **(c)** average amount of water absorbed by each biopolymer composite

3.5 Water Absorption Capacity

The water absorption of the bioplastics after seven days was as follows: SBF (53.26%), CBF1 (25.71%), CBF2 (16.67%), CBF3 (43.75%), CBF4 (38.21%), CBF5 (28.41%), CBF6 (22.14%), CBF7 (6.34) and CBF8 (1.33%). From the results shown in Figure 5, it is observed that with an increase in immersion time, the rate of water absorption increases. However, the more the SiO_2-NPs the more resistant to water absorption. The water absorption of the sample without SiO_2-NPs addition (SBF) is greater because, in the other samples, more hydrogen bonds formed between the SiO_2-NPs and the starch. The implication of this is that it does not allow water molecules to interact freely. Also, other researchers have shown the positive effects of nanoparticles [9].

3.6 Kinetics of Water Absorption

Accurate prediction of moisture content over time is crucial to identify areas prone to cracking in hot, humid conditions [10]. Moisture moves in polymer composites by diffusion, so a robust model is essential. Fick's model is favored for its simplicity; its laws, inspired by heat conduction, effectively analyze moisture absorption data [11]. Diffusion kinetics is described by Equation 4-7.

$$Q_t/Q_{eq} = kt^n \quad (4)$$

$$\log[Q_t/Q_{eq}] = n\log[t] + \log[k] \quad (5)$$

$$Q_t = [(W_t - W_d)/M_{wt}]/W_d * 100 \quad (6)$$

Here, W_t and W_d are the immersed and oven-dried weights, and M_{wt} (≈18.0153 g/mol) is the molar mass of water. Q_t and Q_{eq} (mol%) denote moisture content at time *t* and equilibrium. Equilibrium is reached when weight variations are ≤ 1% (≈0.005 g). Constants k and n capture the polymer structure, water interaction, and transport mechanism. By plotting log (Q_t/Q_{eq}) versus log(*t*), the slope (*n*) and intercept (*k*) for SBF and CBF composites were determined (Figure 6 and Table 2); notably, only CBF7 had $n \approx 0.5$, indicative of Fickian diffusion. Experimental data like water absorption often require normalization. Equation 7 normalizes values, where $y_{normalized}$ is the result, and y_{min} and y_{max} are the minimum and maximum of *y*, respectively.

$$y_{normalized} = 0.05 + 0.85 * \{(y - 0.95y_{min})/(1.05y_{max} - 0.95y_{min})\} \quad (7)$$

This approach effectively links the kinetics of moisture absorption with the material's behavior under varying conditions [12].

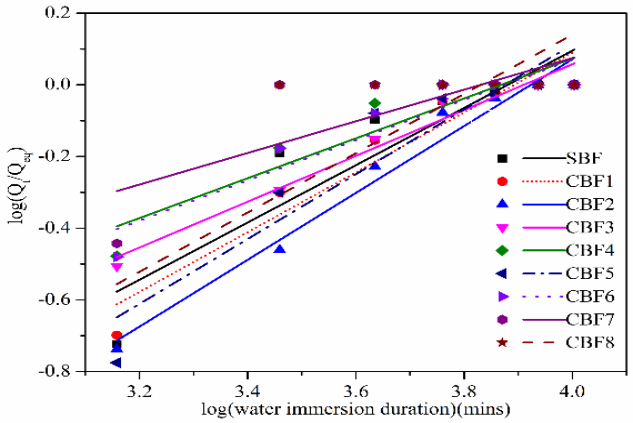

Figure 6: Linear regression for evaluation of diffusion parameters *n* and *k*

Table 2: Water absorption diffusion constants: *k* and *n*

Composite	*k*	*n*	Adj. R^2
SBF	-3.1006	0.79899	0.80313
CBF1	-3.24697	0.8341	0.91115
CBF2	-3.65952	0.93277	0.96254
CBF3	-2.49953	0.63926	0.95314
CBF4	-2.15234	0.55642	0.83441
CBF5	-3.50522	0.90441	0.85001
CBF6	-2.17812	0.56218	0.85587
CBF7	-1.68971	0.4411	0.53797
CBF8	-3.16906	0.8273	0.53797

3.7 Fourier Transform Infrared Spectroscopy Test

FTIR identified functional groups and chemical changes from plasticizers and fillers, enabling rapid analysis [13]. Changes in characteristic bands indicate physical versus chemical interactions when substances mix. The FTIR spectra (Figure 7) show absorption signals for all key biopolymer groups. A prominent -C-O peak was observed at 928.1 cm^{-1} in sample one. Jumaidin *et al.* [14] reported similar peaks (928–1080.9 cm^{-1}) attributed to the anhydrous-glucose ring and C-O stretch from C-O-H groups in starch. Peaks from 2927.7 to 2933.4 cm^{-1}, assigned to the -CH group, indicate hydrocarbon chains. Ongdeesoontorn et al. [15] noted weak C-H stretches at 2927 and 2869 cm^{-1}. An absorption band for C-O-H bending appeared between 1148 and 1151.7 cm^{-1}; differences in peak intensities at 2931 and 1154 cm^{-1} [16] suggest electrostatic interactions between starch and silicon dioxide.

Peaks for -OH groups on the potato starch backbone appeared between 3268.6 and 3272.6 cm^{-1}. As noted by [17], these represent hydrogen-linked hydroxyl clusters that promote intermolecular hydrogen bonding among starch, glycerin, and other film components. This also indicates increased hydrogen bonding between SiO_2 and plastic hydroxyl groups. Hydroxyl groups strongly bind water; initially, adsorbed water is held until saturation [18]. Peaks between 1613.9 and 1640 cm^{-1} correspond to H-O-H stretching, consistent with a peak at 1650 cm^{-1} [19]. Peaks at 1080.9 and 988.9 cm^{-1} result from Si-C stretching and bending, while those at 1072 and 922 cm^{-1} are due to Si–O stretching and Si–H bending [20], indicating enhanced hydrogen bonding between SiO_2-NPs and potato starch. O-Si-O vibrations appeared between 857.3 and 861.0 cm^{-1}. FTIR confirmed the presence of starch and SiO_2-NPs functional groups in both native and modified films. The additional peaks from SiO_2-NPs verify successful starch modification.

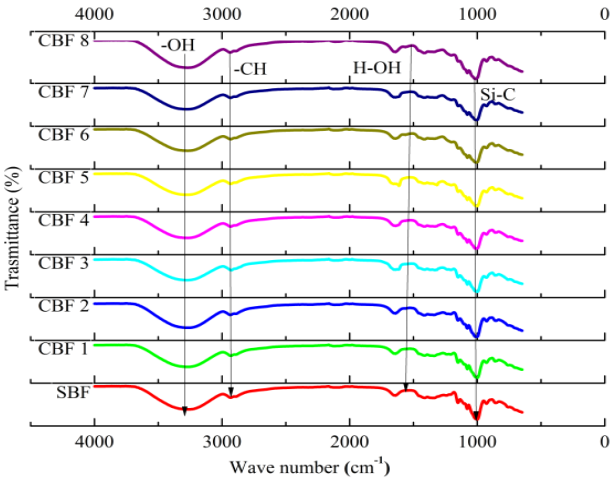

Figure 7: FTIR spectra of bioplastic films

Peaks identified between 1613.9 and 1640 cm^{-1} can be ascribed to H-O-H stretching. A similar report [19] confirmed this where the peak was identified at 1650 cm^{-1}. The Si-C stretching and bending vibrations were responsible for the peaks at 1080.9 and 988.9 cm^{-1}. According to [20], the peaks at 1072 and 922 cm^{-1} were credited to the Si–O stretching vibration and Si–H bending vibration. It showed that the intermolecular hydrogen bonding between SiO_2-NPs and potato starch had increased. Stretching and bending vibrations of O-Si-O were observed between 857.3 cm^{-1} and 861.0 cm^{-1}. The FTIR analysis confirmed the presence of functional groups in both the native and modified starch films. It revealed characteristic peaks corresponding to the starch components and the SiO_2-NPs. Notably, the FTIR results suggested that incorporating SiO_2-NPs resulted in additional peaks, indicating the successful modification of the starch.

3.8 Thermogravimetric Analysis (TGA)

Thermogravimetric analysis (TGA) examined the films' thermal degradation per ASTM E1131-08 using a PerkinElmer TGA 4000 (Netherlands). Figure 8 shows TGA effectively tracks decomposition via mass

changes with temperature. Thermal decomposition refers to mass loss from rising temperature, revealing structural changes, polymer morphology, additive reactions, and filler interactions [21]. Starch-based bioplastic degradation occurs in three stages. In Stage 1 (25–300 °C), moisture and light volatiles (such as acetic acid) evaporate, causing ~10% weight loss in starch films, while SiO_2-NPs/potato starch films lose less, indicating nano-SiO_2 hinders water movement [22].

Stage 2 (300–500 °C) sees volatile release and complete glycerol evaporation near 400 °C, with 60–80% weight loss due to hydroxyl elimination and glycosidic bond rupture [23]. Pure potato starch films lose about 85.1% of weight, whereas composite films lose less than 85%, as interactions between starch and Si-OH in SiO_2-NPs delay chain movement and enhance thermostability [24]. Stage 3 (500–900 °C) involves the release of remaining volatiles and carbon loss [25], aligning with FTIR results. In a nutshell, incorporating SiO_2-NPs raises degradation temperatures and improves the films' thermal stability.

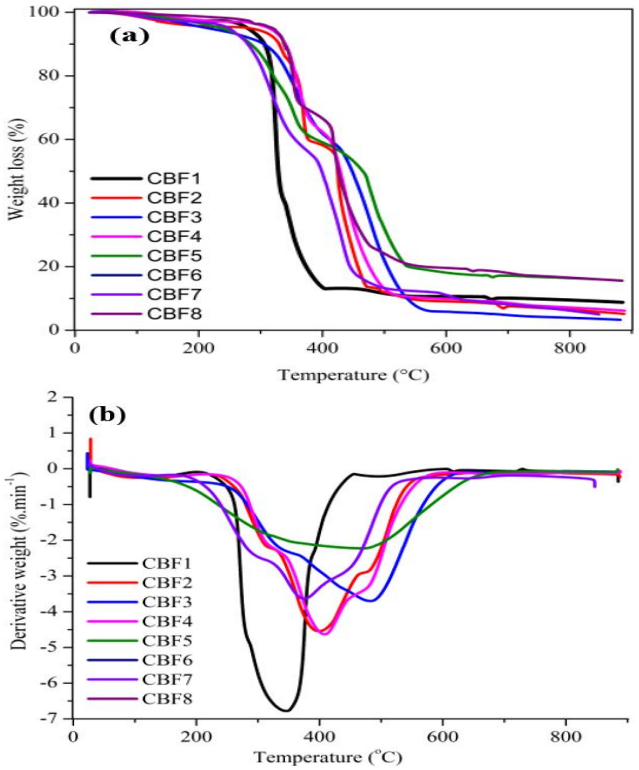

Figure 8: Curves representing temperature distribution of **(a)** TGA and **(b)** DTG for biopolymer film composites: CBF1 to CBF8 with varied proportions of SiO_2-NPs additions

3.9 Biodegradability Test

The examination of the data presented in the graph reveals a noteworthy pattern in the behaviour of bioplastic films concerning water absorption (Figure 9). Notably, during the initial seven days, all the bioplastic films exhibited a consistent uptake of water. However, a pivotal shift occurred after this duration, as the films commenced releasing the absorbed water, consequently initiating a decline in their overall weight. This decrement persisted until the films reached their saturation point. The data indicates an initial phase where the samples absorbed water up till the seventh day, followed by a steady increase in weight reduction as the days progressed. Remarkably, after 14 days, a significant percentage of weight loss 94.5 % for starch bioplastic and 60.1 % for composite bioplastic—was recorded, suggesting a continuous deterioration over time. This aligns with the findings of Tunma et al. [26], who observed the complete decomposition of starch-based films, with or without nanoparticles, within 14 days. This test shows that the bioplastic films can biodegrade in a wet environment if exposed for a long period, without the soil burial. The biodegradability test results showed that the native starch film exhibited significantly greater biodegradability than the SiO_2-NPs modified films. However, all films exhibited higher biodegradability compared to conventional polyethylene films.

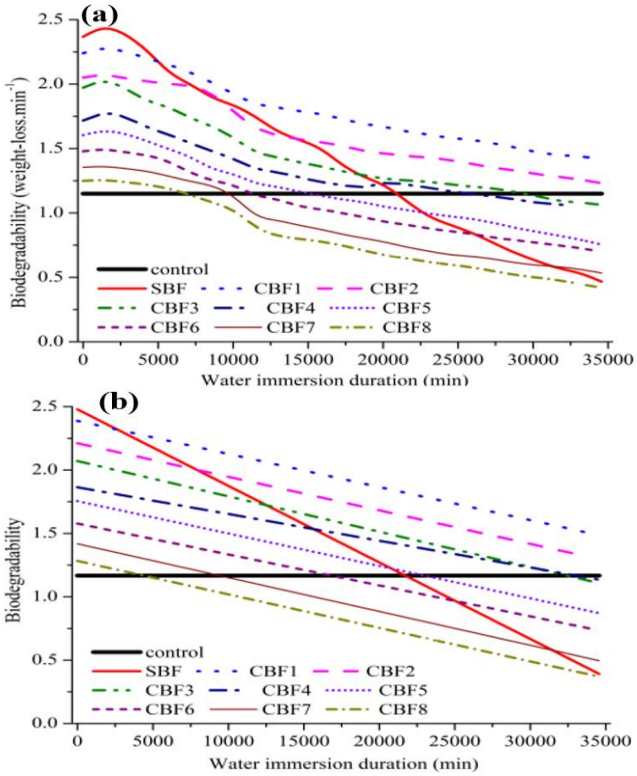

Figure 9: The rate of biodegradation of biopolymer film composites: **(a)** quasi-linear correlation, and **(b)** linear correlation

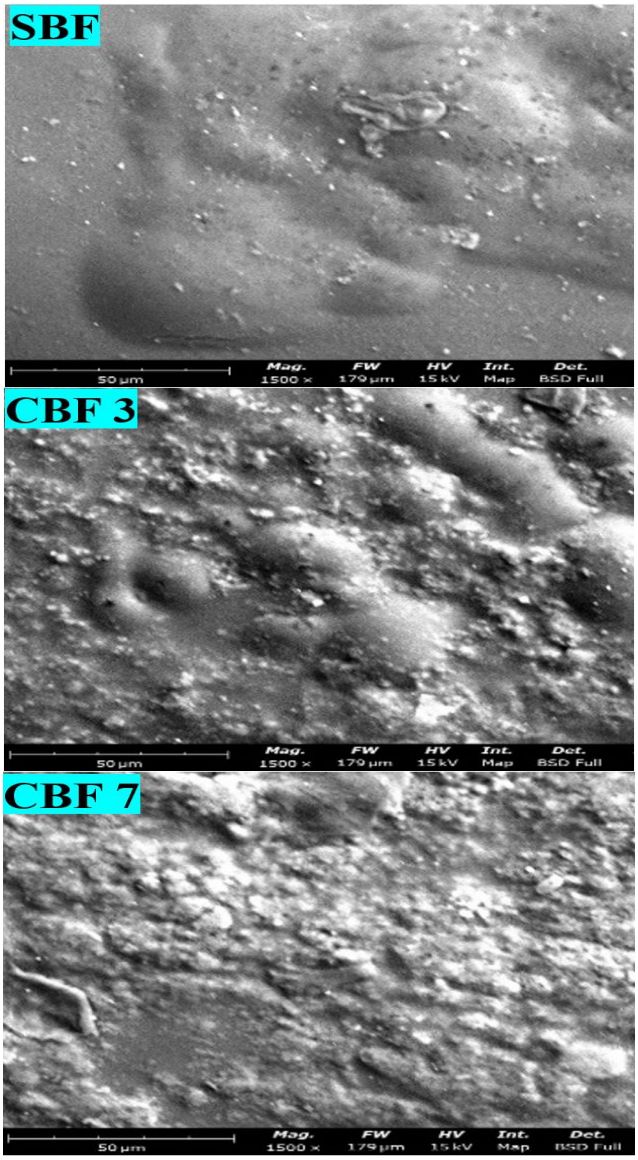

Figure 10: The morphology of SBF, and CBFs (1-8) biopolymer film composites

3.10 Morphological Examination of Biopolymer Films

Morphological analysis was conducted using SEM following ASTM E766-14e1 (Figure 10). The surface topography reveals key traits of these biodegradable films. Micrographs show that the native potato starch film (SBF) is smoother than films with SiO_2-NPs. Increased SiO_2-NPs concentration leads to greater surface roughness. This agrees with Hernádez et al. [27], who observed swelling of undissolved starch granules. CBF composite films contain more residual starch and non-gelatinized SiO_2-NPs than starch-only films. SiO_2-NPs addition increases roughness and reduces uniformity, as linked to nanoparticle distribution, Lizundia et al. [28]. Microscopic inspection also revealed voids, edges, gaps, and poor bonding. Fewer cracks in composite films suggest better component bonding. Voids contribute to lower impact and tensile strength, aligning with Raudah et al. [29] on incompatible blends. Compared to starch-only films, CBF composites show fewer voids, holes, and cracks, indicating improved compatibility, Amin et al. [3]. The rougher surfaces in modified films, due to SiO_2-NPs, may affect water absorption.

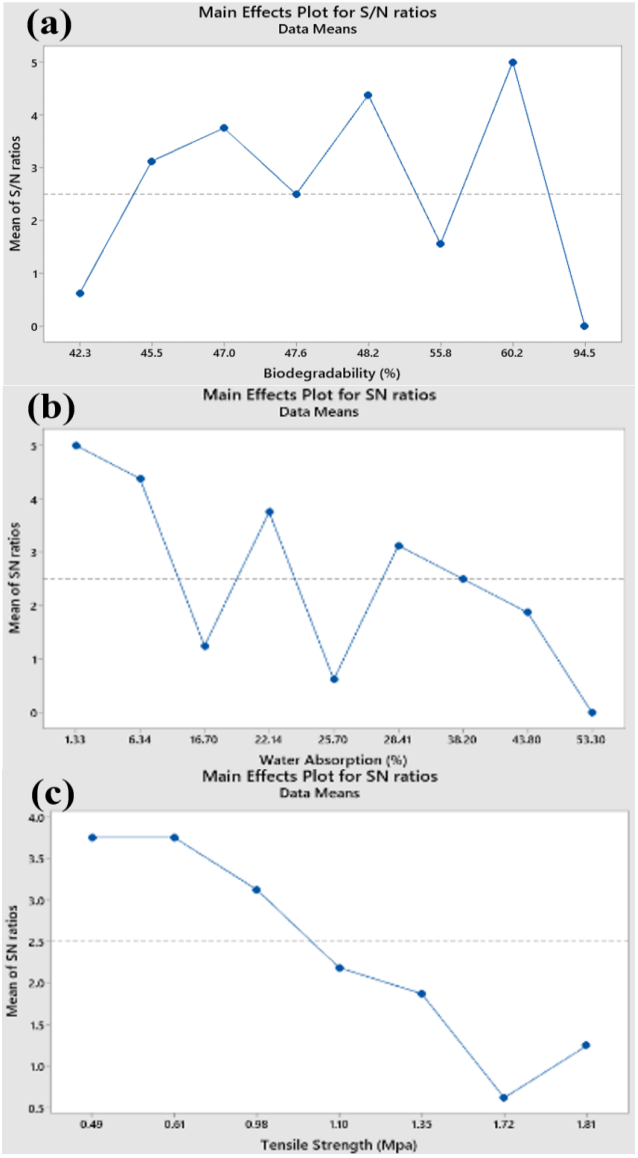

Figure 11: SN ratios of data mean for **(a)** biodegradability, **(b)** water absorption, and **(c)** tensile strength

3.11 Response Optimization and Signal to Noise Ratio (S/N)

Mixture design (extreme vertices) was employed in this project to create the design of the experiment. The composite biopolymer sample with the highest fit is considered the optimal sample and the sample with 14.375g of starch and 0.625g of SiO_2-NPs has the highest fit in terms of tensile strength, water absorption, and biodegradability. The Analysis of Variance (ANOVA) fit results were translated into a

main effect plot. The main effect plot depicts each parameter's effect at various levels. Figures 11 (a, b, and c) show the main effect plots were calculated, in which it was observed that minimum starch and minimum SiO_2-NPs give the optimal properties.

The response optimizer utilized Derringer-modified Harrington's desirability function approach for multi-response multi-factor optimization of response models. This approach furnishes a combination of factor settings that concurrently optimize a set of responses and define the optimal settings for addressing a collection of multivariate objective functions. As seen in Table 3 this optimization is based on the concept of maximizing the response.

Table 3: Multi-response prediction summary

Response	Fit	SE Fit	95% CI	95% PI
Biodegradability (%)	49.66	5.34	(35.92, 63.39)	(27.34, 71.97)
Water Absorption (%)	23.27	6.61	(6.29, 40.25)	(-4.31, 50.86)
Tensile Strength (MPa)	1.809	0.278	(1.093, 2.525)	(0.646, 2.972)

With the aid of a response optimizer, the maximum responses for water absorption, biodegradability, and tensile strength were 38.3521 %, 66.2897 %, and 1.41433 MPa respectively, with a composite desirability of 0.612029.

3.12 Response Surface Plots

Individual and cumulative influences of the factors on the dependent variable as well as mutual interactions between the factors were depicted using response surface plots. The response surface regression is presented in Equations 8-10, for tensile strength, water absorption, and biodegradability

Tensile strength (MPa) = 1.05 + 0.471 (Starch) + 0.078 (Starch * SiO_2-NPs) (8)

Water Absorption (%) = 30.17 + 18.03 (Starch) + 9.5 (Starch * SiO_2-NPs) (9)

Biodegradability (%) = 44.62 + 9.83 (Starch) – 25.4 (Starch * SiO_2-NPs) (10)

Figure 12a shows that biodegradability increases with SiO_2-NPs and decreases with starch. The highest biodegradability (70%) occurs at 13-14% SiO_2-NPs and 1-2% starch. The optimum is 13–14% SiO_2-NPs with 1–2% starch, with biodegradability ranging from 10% to 70%. Adjusting these levels control biodegradability. Similarly, Figure 12b reveals that water absorption peaks at 0-1% SiO_2-NPs and 13-14% starch; it decreases rapidly above 1% SiO_2-NPs or below 13% starch. Starch has a greater effect on water absorption than SiO_2-NPs, as indicated by the steeper slope in the starch direction. It also indicated that water absorption rises with more SiO_2-NPs and less starch. The highest absorption (20–60%) occurs at 0–1% SiO_2-NPs and 13–14% starch, with starch having a larger impact. Figure 12c demonstrates that tensile strength increases with SiO_2-NPs and decreases with starch, reaching the highest and best strength value (1.6 MPa) at 13-14% SiO_2-NPs and 1-2% starch. Below 3% SiO_2-NPs, tensile strength drops quickly. The tensile strength is primarily determined by the total SiO_2-NPs and starch amounts, not their ratio, as seen from the surface plot's symmetry. It also shows that the response is nearly symmetrical, showing total content matters more than ratio, and SiO_2-NPs influence strength more. Biodegradability, water absorption, and tensile strength are mainly determined by the total amounts of SiO_2-NPs and starch levels rather than their specific ratio or proportion.

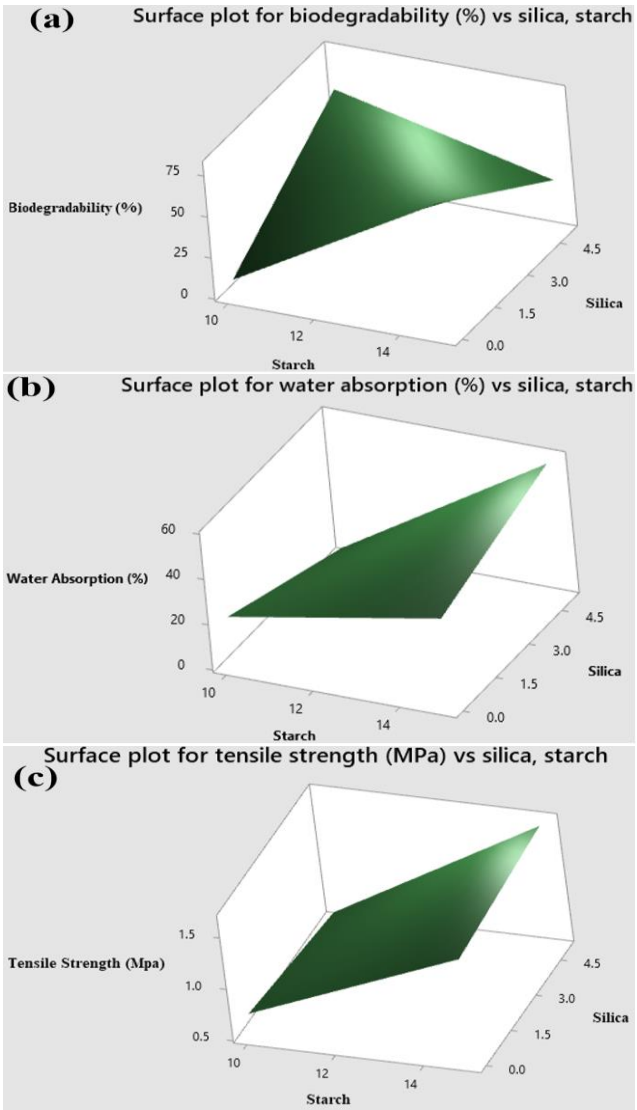

Figure 12: 3D response surface plot of varied amounts of starch, SiO_2-NPs, biodegradability

(a), Water absorption **(b)**, and Tensile strength **(c)** of biopolymer films produced

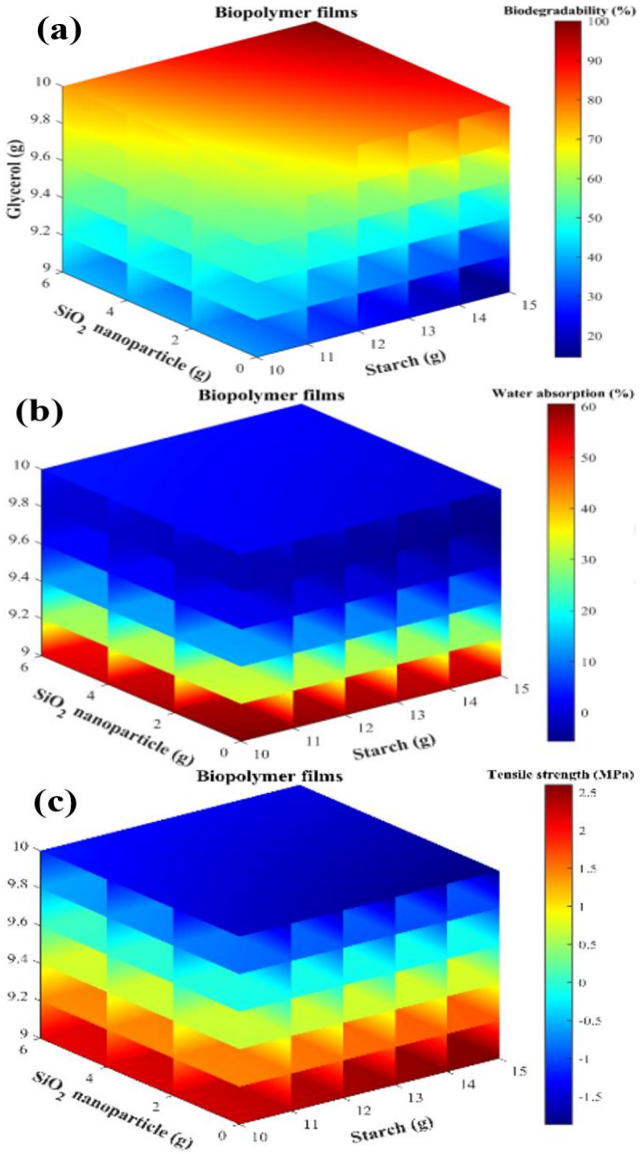

Figure 13: 3D mapping of varied amounts of starch, SiO_2-NPs, and optimized signal-to-noise ratio for: **(a)** biodegradability, **(b)** Water absorption, and **(c)** Tensile strength of biopolymer films produced

3.13 Mapping of Biodegradability, Water Absorption, and Tensile Properties of Bioplastic Films

Figure 13a shows biodegradability drops with higher starch. For example, a film with 11 g starch, 9.15 g glycerol, and 2 g SiO_2 has 9.8% biodegradability, while one with 13 g starch, 9.15 g glycerol, and 1.2 g SiO_2 has 9.2%. For a given starch level, more glycerol reduces biodegradability; for constant glycerol, more SiO_2 also lowers it. Thus, adjusting these components tailor biodegradability, in which high starch with low SiO_2 yields compostable films, whereas low starch with high SiO_2 produces more durable, antimicrobial films. Figure 13b reveals water absorption increases with starch and glycerol, as starch attracts water. A film with 13 g starch, 9.15 g glycerol, and 2 g SiO_2 absorbs 70% water, while one with 11 g starch, 9.15 g glycerol, and 1.2 g SiO_2 absorbs 65%. Therefore, increasing SiO_2 lowers water uptake. This lets designers meet specific needs: high absorption for food packaging and low absorption for medical devices. Figure 13c indicates tensile strength improves with more SiO_2 but declines with higher starch and glycerol. The best tensile properties (1.5 MPa, 2.5 GPa modulus) occur at 11 g starch, 9.9 g glycerol, and 5.5 g SiO_2; the worst (0.5 MPa, 1.5 GPa) at 13 g starch, 10 g glycerol, and 2 g SiO_2. Thus, lowering glycerol and increasing SiO_2 enhances strength. By tweaking composition, one can balance biodegradability, water absorption, and tensile properties for targeted applications.

4.0 CONCLUSION

This study showed that adding SiO_2-NPs to sweet potato starch improves bioplastic film properties. Films gained in density, water resistance, and tensile strength. SiO_2-NPs reduced water penetration by about 40%. However, tensile strength (0.49–1.81 MPa) remained lower than in conventional polymers (15–17 MPa), which could limit the applications. FTIR confirmed key functional groups (-OH, -CO, -CH, -C-O, H-O-H, Si-O, Si-H). TGA revealed that composite films degrade slower than pure starch films, indicating better thermal stability. SEM images showed more residual starch and SiO_2-NPs granules in composites. SiO_2-NPs increased surface roughness while reducing uniformity. Biodegradability tests indicated that pure starch films degrade faster than composites, though both are highly biodegradable, unlike polyethylene controls which showed no change. Optimization pinpointed 0.625 g SiO_2-NPs and 13.275 g starch as ideal. In summary, starch-based bioplastics are more biodegradable than LDPE/HDPE. SiO_2-NPs enhanced tensile properties and water resistance, yet their use in food packaging remained limited. Future research should focus on adding fire-resistant fillers or mixing starch with flame retardants, as starch's porous structure promotes rapid gas movement and melting.

CONFLICTS OF INTEREST

No conflict of interest was declared by the authors.

REFERENCES

[1] Karan, H., Funk, C., Grabert, M., Oey, M., and Hankamer, B. "Green bioplastics as part of a circular bioeconomy", *Trends in plant science*,

Vol. 24, no. 3, pp.237-249, 2019. https://doi.org/10.1016/j.tplants.2018.11.010.

[2] Ebhota, W. S., and Tabakov, P. Y. "Leveraging agrivoltaics to increase food, energy, and water access in the global south: a case study sub-Carnahan Africa", *Nigerian Journal of Technology*, Vol. 43, no. 2, 2024. https://doi.org/10.4314/njt.v43i2.20.

[3] Amin, M. R., Chowdhury, M. A., and Kowser, M. A. "Characterization and performance analysis of composite bioplastics synthesized using titanium dioxide nanoparticles with corn starch", *Heliyon*, Vol. 5, no. 8, pp.1-12, 2019, e02009. https://doi.org/10.1016/j.heliyon.2019.e02009.

[4] Onovo, H. O., Agbeleye, A. A., Akano, T. T., Oludele, D. B., Olawoyin, J. O., and Kentosu, I. S. "Comprehensive Study of Extraction and Applicability of Nanosilicate Particles from Natural Waste for Biopolymer Reinforcement", *Nigerian Journal of Technology*, Vol. 43, no. 4, pp.666–675, 2024. https://doi.org/10.4314/njt.v43i4.7.

[5] Khoramnejadian, S., Zavareh, J. J., and Khoramnejadian, S. "Effect of potato starch on thermal and mechanical properties on low-density polyethylene", *Current World Environment*, Vol. 8, no. 2, pp.215-220, 2013. http://dx.doi.org/10.12944/CWE.8.2.06.

[6] "What is Starch?" Accessed Jan 21, 2025, from https://byjus.com/chemistry/starch/#uses-of-starch.

[7] "Scilab 2024.0.0." Accessed October 30, 2024 from https://www.scilab.org/download/scilab-2024.0.0.

[8] Onovo, H. O., Akano, T. T., Onyegbule, D. U., Towolawi, E. T., and Ajala, T. S. "A study of Biodegradation of Hybrid Bioplastic Films Blend from Manihot and Triticum Biopolymer", *European Journal of Engineering and Technology Research*, Vol. 7, no. 3, pp.30-38, 2022. http://dx.doi.org/10.24018/ejeng.2022.7.3.2772.

[9] Sultan, N. F. K., and Johari, W. L. W. "The development of banana peel/corn starch bioplastic film: a preliminary study", *Bioremediation Science and Technology Research*, Vol. 5, no. 1, pp.12-17, 2017. https://doi.org/10.54987/bstr.v5i1.352.

[10] Voon, H. C., Bhat, R., Easa, A. M., Liong, M. T., and Karim, A. A. "Effect of Addition of Halloysite Nanoclay and SiO_2 Nanoparticles on Barrier and Mechanical Properties of Bovine Gelatin Films", *Food Bioprocess Technology*, Vol. 5, no. 5, pp.1766–1774, 2012. https://doi.org/10.1007/s11947-010-0461-y.

[11] Ruth, A. L-A., Aziz, H., Yahya, R., Abd Rahman, N., and Fauzani Md, S. "Water absorption behavior of heat-treated and untreated red balau saw dust/LDPE composites: Its kinetics and effects on mechanical properties", *Journal of Thermoplastic Composite Materials*, pp.1–19, 2018. https://doi.org/10.1177/0892705718799823.

[12] Munde, Y., Shinde, A., Anerao, P., and Siva, I. "Identifying the Effect of Stacking Sequence on Water Absorption, Mechanical and Fracture Properties of Flax/Glass Hybrid Composites", *Proceedings of the International Symposium on Lightweight and Sustainable Polymeric Materials (LSPM23), Springer Proceedings in Materials*, Vol. 32, 2023. https://doi.org/10.1007/978-981-99-5567-1_19.

[13] Manaila, E., Craciun, G., Ighigeanu, D., and Stelescu, M. D. "Water Absorption Kinetics in Composites Degraded by the Radiation Technique", *Materials*, Vol. 14, 2021, 4659. https://doi.org/10.3390/ma14164659.

[14] Joliff, Y., Belec, L., and Chailan, J. F. "Modified water diffusion kinetics in an unidirectional glass/fiber composite due to the interphase area: Experimental, analytical and numerical approach", *Composite Structures*, Vol. 97, pp.296–303, 2013. https://doi.org/10.1016/j.compstruct.2012.09.044.

[15] Bond, D. A. "Moisture Diffusion in a fiber-reinforced composite: Part I—Non-Fickian transport and the effect of fiber spatial distribution", *Journal of Composite Materials*, Vol. 39, pp.2113–2141, 2004. https://doi.org/10.1177/0021998305052030.

[16] Pavia, S., Walker, R., Veale, P., and Wood, A. "Impact of the properties and reactivity of rice husk ash on lime mortar properties", *Journal of Materials in Civil Engineering*, Vol. 26, no. 9, pp.1-8, 2014, 04014066, https://doi.org/10.1061/(ASCE)MT.1943-5533.0000967.

[17] Jumaidin, R., Sapuan, S. M., Jawaid, M., Ishak, M. R., and Sahari, J. "Characteristics of thermoplastic sugar palm Starch/Agar blend: Thermal, tensile, and physical properties", *International journal of biological macromolecules*, Vol. 89, pp.575-581, 2016, https://doi.org/10.1016/j.ijbiomac.2016.05.028.

[18] Tongdeesoontorn, W., Mauer, L. J., Wongruong, S., Sriburi, P., Rachtanapun, P. "Effect of carboxymethyl cellulose concentration on physical properties of biodegradable cassava starch-based films",

Chemistry Central Journal, Vol. 5, no.1, pp.1-8, 2011. https://doi.org/10.1186/1752-153X-5-6.

[19] Olayaei, S. A., Almasi, H., Ghanbarzadeh, B., and Moayedi, A. A. "The synergistic reinforcing effect of TiO2 and montmorillonite on potato starch nanocomposite films: Thermal, mechanical and barrier properties", *Carbohydrate Polymers*, Vol. 152, no. 5, pp.53-262, 2016, https://doi.org/10.1016/j.carbpol.2016.07.040.

[20] Obasi, H. C. "Tensile and biodegradable properties of extruded sorghum flour filled high density polyethylene films", *Academic Research International*, Vol. 4, no. 5, pp.78-86, 2013.

[21] Zhang, R., Wang, X., and Cheng, M. "Preparation and characterization of Potato Starch Film with various size of Nano-SiO_2", *Polymers*, Vol. 10, no. 10, 2018, 1172. https://doi.org/10.3390/polym10101172.

[22] Jiang, S. S., Liu, C. Z., Wang, X. J., Xiong, L., and Sun, Q. J. "Physicochemical properties of starch nanocomposite films enhanced by self-assembled potato starch nanoparticles", *LWT - Food Science and Technology*, Vol. 69, pp.251-257, 2016. https://doi.org/10.1016/j.lwt.2016.01.053.

[23] Zhang, R., Cheng, M., Wang, X., and Wang, J. "Bioactive mesoporous nano-silica/potato starch films against molds commonly found in post-harvest white mushrooms", *Food Hydrocolloids*, Vol. 95, pp.517-525, 2019. https://doi.org/10.1016/j.foodhyd.2019.04.060.

[24] Zhao, Y. L., Qi, X. W., Dong, Y., Ma, J., Zhang, Q., Song, L., Yang, Y., and Yang, Q. "Mechanical, thermal and tribological properties of polyimide/nano-SiO2 composites synthesized using an in-situ polymerization", *Tribology International*, Vol. 103, pp.599-608, 2016. https://doi.org/10.1016/j.triboint.2016.08.018.

[25] Shahabi-Ghahfarrokhi, I., Khodaiyan, F., Mousavi, M., and Yousefi, H. "Preparation of UV-protective kefiran/Nano-ZnO nanocomposite: physical and mechanical properties", *International Journal of Biological Macromolecules*, Vol. 72, pp.41-46, 2015. https://doi.org/10.1016/j.ijbiomac.2014.07.047

[26] Kristo, E., and Biliaderis, C. G. "Physical properties of starch nanocrystal-reinforced pullulan films", *Carbohydrate Polymers*, Vol. 68, pp.146-158, 2007. https://doi.org/10.1016/j.carbpol.2006.07.021.

[27] Tunma, S. "Starch-based nanocomposites in active packaging for extended shelf life of fresh fruits", *Walailak Journal of Science and Technology (WJST)*, Vol. 15, no. 4, pp.273-281, 2017. https://doi.org/10.48048/wjst.2018.3849

[28] Hern'andez-Jaimes, C., Meraz, M., and Lara, V. H. "Acid hydrolysis of composites based on corn starch and trimethylene glycol as plasticizer", *Revista Mexicana de Ingeniería Química*, Vol. 16, no. 1, pp.169-178, 2017. https://doi.org/10.24275/rmiq/Alim764.

[29] Harunsyah, S. R. "The effect of clay nanoparticles as reinforcement on mechanical properties of bioplastic base on cassava starch", *Journal of Physics: Conference series*, Vol. 1, 953., 2018. https://doi.org/10.1088/1742-6596/953/1/012021.